

Bogdan Iorga · Denyse Herlem ·  
Elvina Barré · Catherine Guillou

## Acetylcholine nicotinic receptors: finding the putative binding site of allosteric modulators using the “blind docking” approach

Received: 5 April 2005 / Accepted: 9 August 2005 / Published online: 22 December 2005  
© Springer-Verlag 2005

**Abstract** Allosteric potentiation of acetylcholine nicotinic receptors is considered to be one of the most promising approaches for the treatment of Alzheimer’s disease. However, the exact localization of the allosteric binding site and the potentiation mechanism at the molecular level are presently unknown. We have performed the “blind docking” of three known allosteric modulators (galanthamine, codeine and eserine) with the Acetylcholine Binding Protein and models of human  $\alpha 7$ ,  $\alpha 3\beta 4$  and  $\alpha 4\beta 2$  nicotinic receptors, created by homology modeling. Three putative binding sites were identified in the channel pore, each one showing different affinities for the ligands. One of these sites is localized opposite to the agonist binding site and is probably implicated in the potentiation process. On the basis of these results, a possible mechanism for nicotinic acetylcholine receptor (nAChRs) activation is proposed. The present findings may represent an important advance for understanding the allosteric modulation mechanism of nAChRs.

**Keywords** Allosteric modulators · Acetylcholine nicotinic receptors · Docking

### Introduction

Alzheimer’s disease (AD) [1, 2] is the most common form of degenerative dementia of the human central nervous

system characterized by progressive memory loss, disorientation, and pathological markers (senile plaques and neurofibrillary tangles) [3]. The main existing treatments for AD are the inhibition of acetylcholinesterase (AChE) [4, 5] and the blocking of NMDA receptors [6]. Presently, three acetylcholinesterase inhibitors (AChEIs) are available on the market: donepezil (Aricept), rivastigmine (Exelon) and galanthamine (Reminyl). Memantine (Ebixa), an NMDA receptor antagonist, is the latest drug released for the treatment of AD.

An interesting alternative for the treatment of AD has emerged in recent years. Indeed, the allosteric modulation of nicotinic acetylcholine receptors (nAChRs) appears as a new, promising approach for the treatment of this disease [7–17]. As the allosteric modulators do not interact with the agonist binding site, the secondary effects due to receptor desensitization observed for the nAChR agonists are expected to be suppressed [13].

Nicotinic acetylcholine receptors are pentameric membrane proteins traditionally classified into “muscle” and “neuronal” types. The “muscle” nAChRs are heteropentamers with the stoichiometry  $(\alpha 1)_2(\beta 1)\gamma\delta$  prior to innervation and  $(\alpha 1)_2(\beta 1)\delta\varepsilon$  after innervation. The “neuronal” nAChRs can be classified, based on their subunit composition, in two subtypes: homopentamers consisting of  $\alpha 7$ – $\alpha 10$  subunits and heteropentamers consisting of various combinations of  $\alpha 2$ – $\alpha 6$  and  $\beta 2$ – $\beta 4$  subunits. These subunit combinations confer specific pharmacologies to the nAChRs [18].

The generally accepted mechanism for cholinergic neurotransmission implies the binding of ACh to the amino-terminal domains of nAChRs, which undergo conformational changes that trigger the opening of the ion channel (gating mechanism). The fixation of an allosteric modulator induces an apparent enhancement of receptor affinity and increases the probability of channel opening. Three different conformations of the nAChRs have been postulated, based on the Monod–Wyman–Changeux model of allosteric transitions: the open, closed and desensitized states [19]. A number of hypotheses concerning the channel-opening mechanism have been proposed [20–27] on the basis of the recently published cryo-electron microscopy

**Electronic Supplementary Material** Supplementary material is available for this article at <http://dx.doi.org/10.1007/s00894-005-0057-z>

B. Iorga (✉) · D. Herlem ·  
E. Barré · C. Guillou (✉)  
Institut de Chimie des Substances Naturelles,  
CNRS UPR 2301, Avenue de la Terrasse,  
F-91198, Gif-sur-Yvette, France  
e-mail: Bogdan.Iorga@icsn.cnrs-gif.fr.  
Tel.: +33-1-69823030  
Fax: +33-1-69077247  
e-mail: Catherine.Guillou@icsn.cnrs-gif.fr.

structures of nAChRs [28, 29]. However, the lack of more precise information on the nAChR three-dimensional structure has limited attempts to gain molecular insight into the ligand-receptor interaction. The publication of the crystal structure of the Acetylcholine Binding Protein (AChBP) [30–33], a soluble protein homologue to the extracellular domain of nAChRs, bound to HEPES [30, 33], nicotine [33] and carbamylcholine [33], changed the situation significantly. In functional terms, AChBP shares virtually all the ligand-binding characteristics with the nicotinic receptor family, and reveals a structure largely consistent with the electron-microscopy image, chemical modification, mutagenesis, and spectroscopic data [34]. Considering its sequence identity with the amino-terminal part of  $\alpha 7$  nAChR (26%) and the similar behavior towards the “classical” nAChR ligands, AChBP is considered as a reliable structure for nAChR homology modeling and docking simulations [35–37]. A number of modeled nAChRs structures have been published in recent years [38–47].

Galanthamine, codeine and eserine (physostigmine) are three known allosteric modulators (allosteric potentiating ligands, APLs) of nAChRs (Fig. 1) [9, 48–50]. Some of them (galanthamine and eserine) show a dual mode of action, also being good AChEIs. This duality confers to galanthamine its effectiveness in the treatment of AD [5, 12, 51]. In addition, APLs can act as non-competitive agonists of very low efficacy, and as direct blockers of ACh-activated channels. These actions are observed with nAChRs from brain, muscle and electric tissue. They depend on the structure of the APL and the concentration range applied [50, 52, 53].

The exact position of the binding site of nAChR APLs is not very clear [54]. Photoaffinity labeling experiments and epitope mapping for the eserine-competitive antibody FK1 have identified the  $\alpha$ Lys125 residue of *Torpedo* nAChR in the allosteric binding site, or in its immediate vicinity [55–57]. These results have been exploited recently [45] for the

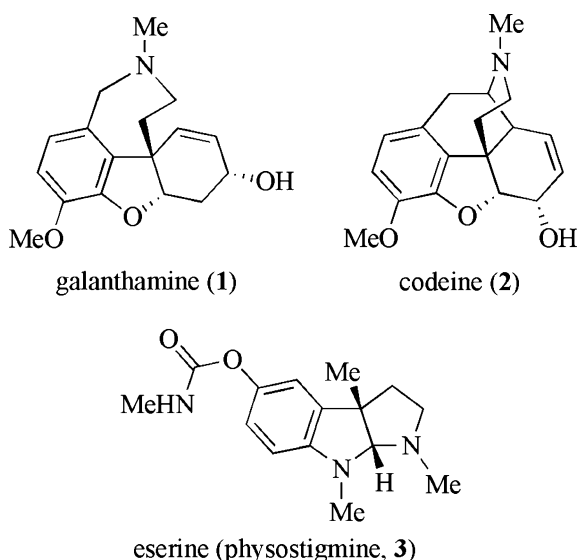


**Fig. 1** Chemical structures of three allosteric modulators of nicotinic acetylcholine receptors

docking of eserine in a region defined within 14Å from  $\alpha$ Lys122 of murine nAChR (corresponding to  $\alpha$ Lys125 of *Torpedo* nAChR) using the DOCK program [58].

In this paper, we present the results of a more general investigation intended to elucidate the location of the allosteric binding site of nAChRs using the “blind docking” approach [59], a powerful feature of the AUTODOCK program [60]. For this purpose, we created models of human  $\alpha 7$ ,  $\alpha 3\beta 4$  and  $\alpha 4\beta 2$  nAChRs on which we docked three allosteric modulators without imposing a binding site. Three binding sites were identified in the channel pore, one of them being located opposite to the agonist binding site. These findings are discussed and a possible interpretation, considering the experimental results previously published, is proposed.

## Materials and methods

### Sequence alignment

The multiple alignment between AChBP and the amino-terminal domains of human  $\alpha 3$ ,  $\alpha 4$ ,  $\alpha 7$ ,  $\beta 2$  and  $\beta 4$  nAChRs subunits was obtained by means of the CLUSTALX package applying the default parameters [61]. The initial alignment was refined further manually.

### Model building

The program MODELLER (version 6v2) [62, 63] was used to build the three-dimensional models of the amino-terminal domains of human  $\alpha 7$ ,  $\alpha 4\beta 2$  and  $\alpha 3\beta 4$  nAChRs according to the comparative protein modeling method. The template used was the X-ray structure of AChBP (2.7Å resolution, PDB entry code 1I9B). To maintain the complementarity between subunits at their interfaces, all five units were modeled simultaneously. As expected, the backbone atoms of the predicted models and AChBP overlapped well (RMSD values computed using CHIMERA [64] are 0.71 Å for  $\alpha 7$ , 0.60 Å for  $\alpha 3\beta 4$  and 0.63 Å for  $\alpha 4\beta 2$ , respectively), due to the algorithm used by MODELLER and to the low number of gaps in the alignment. Additionally, the structures were checked with PROCHECK [65]. The comparison of the Ramachandran plots shows that the models have good quality, with 85–86% of the residues in the most favorable regions (see supplementary material). For the AChBP and  $\alpha 7$  model, the subunit at the clockwise side of each interface as viewed from the N-terminus is called “plus” and the other “minus”.

### Ligand structure

For galanthamine, the coordinates extracted from the X-ray structure of the complex with AChE (PDB entry 1DX6) [66] were used. For codeine and eserine, the coordinates were taken from the Cambridge Structural Database (CSD), entries ZZZTSE01 [67] and ESERIN10 [68], respectively.

The docking of galanthamine, codeine and eserine into AChBP and human  $\alpha 7$ ,  $\alpha 4\beta 2$  and  $\alpha 3\beta 4$  models was performed with the program AUTODOCK (version 3.0.5) [60]. Its graphical front-end, AUTODOCKTOOLS [69], was used to add polar hydrogens and partial charges for proteins and ligands using the Kollman United Atom and Gasteiger charges, respectively. Atomic solvation parameters and fragmental volumes for the proteins were assigned using the ADDSOL tool (included in the program package). Flexible torsions in the ligands were assigned with the AUTOTORS module and all dihedral angles were allowed to rotate freely. In general, these were all acyclic, non-terminal single bonds (excluding amide bonds) in a given ligand molecule. Affinity grid fields were generated using the auxiliary program AUTOGRID.

The genetic algorithm-local search (GA-LS) hybrid was used to perform an automated molecular docking. Default parameters were used, except for the number of generations, energy evaluations, and docking runs, which were set to 1,000, 25,000,000 and 256, respectively. The docking process was performed in two steps. In the first, the docking procedure was applied to the whole protein target, without imposing the binding site (“blind docking”) [59]. The grid field was a 60 Å cube with grid points separated by 1 Å centred at the middle of the protein. In the second step, we docked the ligands in each of the three binding sites found in the first step (“refined docking”). This time, the grid field was a 60 Å cube with grid points separated by 0.3 Å centered on the best scored conformation obtained in the first step. Lennard–Jones parameters 12–10 and 12–6 (supplied with the program package) were used for modeling H-bonds and van der Waals interactions, respectively. The resulting docked conformations were clustered into families of similar binding modes, with a root mean square deviation (RMSD) clustering tolerance of 2 Å. In almost all cases the lowest docking-energy conformations were included in the largest cluster found (which usually contains 80–100% of total conformations). Otherwise, the lowest docking-energy conformations were considered as the most stable orientations. The docking energy represents the sum of the intermolecular energy and the internal energy of the ligand while the free-binding energy is the sum of the intermolecular energy and the torsional free energy [58].

The polar and apolar surface areas of the binding sites were calculated using the GETAREA 1.1 program [70]. The volumes were obtained with the module “SiteID Find Pockets”, part of the SYBYL molecular modeling environment [71], with a 1 Å grid resolution and 3 Å protein film depth, after addition of all hydrogen atoms to the protein. The depth of the binding site was considered as the distance between the most distant spheres generated by the above-mentioned module [71].

## Results and discussion

### Sequence alignment

Although the sequence identity between the AChBP and the human nAChR extracellular domains is relatively low (18–26%, Table 1), the presence of highly conserved ACh binding residues in the AChBP [30] and the nicotinic pharmacology of the AChBP [72] suggest that homology modeling of nAChR extracellular domains using the AChBP structure is appropriate.

The most important requirement in homology modeling is the correct alignment of the sequence to be modeled with that of the template structure. Regions containing insertions relative to AChBP are the greatest sources of uncertainty in modeling [38]. However, only a few insertions are present in our alignment (Fig. 2), situated in non-conserved regions, the modeling program used being designed to accommodate them [73]. Several alignments of nAChRs subunits have been published previously [41–43, 45, 46], our alignment being very similar to those described by Le Novère et al. [41]. The main differences are the residue numbering (our reference is AChBP) and the position of the residues Thr13 and Ala91-Val106, which are shifted one residue lower in our alignment. Henschman et al. [46] used an alignment based on lysine-scanning mutagenesis results, involving one supplementary residue of  $\alpha 7$  nAChRs at the beginning of the alignment. These differences are observed in regions with low sequence identity, so it is difficult to say which alignment is better.

### Model building

We used MODELLER [62, 63] to generate homology models of extracellular domains of human  $\alpha 7$ ,  $\alpha 3\beta 4$  and  $\alpha 4\beta 2$  nAChRs using spatial constraints provided by AChBP (see Materials and methods section). As expected from the model generation algorithm, the output structures do not show major differences with the AChBP structure, as confirmed by the RMSD values for the backbone atoms (0.71 Å, 0.60 Å and 0.63 Å, respectively) and the

**Table 1** Percentage of sequence identities computed using MODELLER software [62, 63] from the alignment shown in Fig. 2

	AChBP	$\alpha 3$ hs	$\alpha 4$ hs	$\alpha 7$ hs	$\beta 2$ hs
$\alpha 3$ hs	21.0 (43)				
$\alpha 4$ hs	20.5 (42)	61.1 (127)			
$\alpha 7$ hs	25.9 (53)	43.2 (89)	44.7 (92)		
$\beta 2$ hs	18.0 (37)	47.8 (99)	52.2 (108)	39.8 (82)	
$\beta 4$ hs	19.5 (40)	47.3 (98)	50.2 (104)	41.7 (86)	70.0 (145)

The number of identical residues is shown in brackets

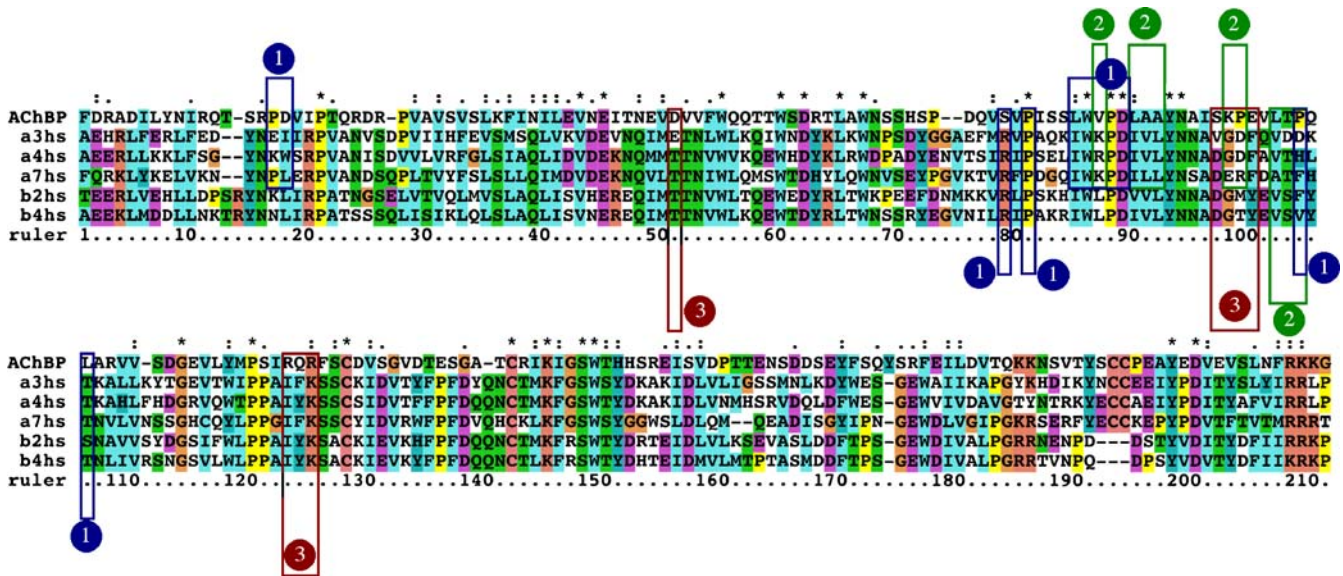


**Fig. 2** Multiple sequence alignment between AChBP and amino-terminal domains of human  $\alpha 3$ ,  $\alpha 4$ ,  $\alpha 7$ ,  $\beta 2$  and  $\beta 4$  nAChRs subunits, represented with CLUSTALX [61, 78]. The stars (\*) represent the fully conserved residues, while the dots (:) and (.)

represent “strongly” and “weakly” conserved residues, respectively. The boxes represent the most important residues of the three allosteric sites: 1 (blue), 2 (green) and 3 (red). See Tables S1–S3 (Supplementary material) for more detailed information

Ramachandran plots (see supplementary material). These results are in good accord with those previously reported for the chick  $\alpha 7$  model [41].

#### Molecular docking

The AUTODOCK program [60] is one of the most reliable docking tools available today, owing its efficiency to the use of a genetic algorithm and to a scoring function comprising several terms (dispersion/repulsion energy, directional hydrogen bonding, screened Coulomb potential electrostatics, a volume-based solvation term, and a weighted sum of torsional degrees of freedom to estimate the entropic cost of binding) [41]. Furthermore, it allows the docking of ligands on the entire protein surface, without prior specification of the binding site (“blind docking”). A parameter set based on the AMBER force field [74] and the possibility of using flexible as well as fixed torsions for the ligands during the docking procedure make AUTODOCK an appropriate tool for this purpose [59].

The docking of three known allosteric modulators of nAChRs (galanthamine, codeine and eserine) with AChBP and the models of human  $\alpha 7$ ,  $\alpha 3\beta 4$  and  $\alpha 4\beta 2$  nAChRs generated before was performed in two steps.

#### “Blind docking”

In the first step, the “blind docking” approach was used in order to identify the potential fixation sites of nAChRs. The resulting conformations of ligands were clustered (RMSD 2 Å) and most of them were found to be located in the channel pore, distributed over three main sites (Fig. 3). The

first one is located between the L1 and L4 loops ( $\alpha/+$  subunit) and the  $\beta 3$  and  $\beta 5$  sheets ( $\beta/-$  subunit) and the most important residues are those corresponding to Pro16, Asp17, Leu81, Trp82, Val83, Pro84 and Asp85 ( $\alpha/+$  subunit) and Ser75, Pro77, Pro100 and Leu102 ( $\beta/-$  subunit) of AChBP. The second site is situated between the loops L4 ( $\alpha/+$  subunit) and L5 ( $\beta/-$  subunit), the conserved residues being those corresponding to Val83, Leu86, Ala87, Ala88, Lys94 and Pro95 ( $\alpha/+$  subunit) and Leu98, Thr99 and Pro100 ( $\beta/-$  subunit) of AChBP. The third one is

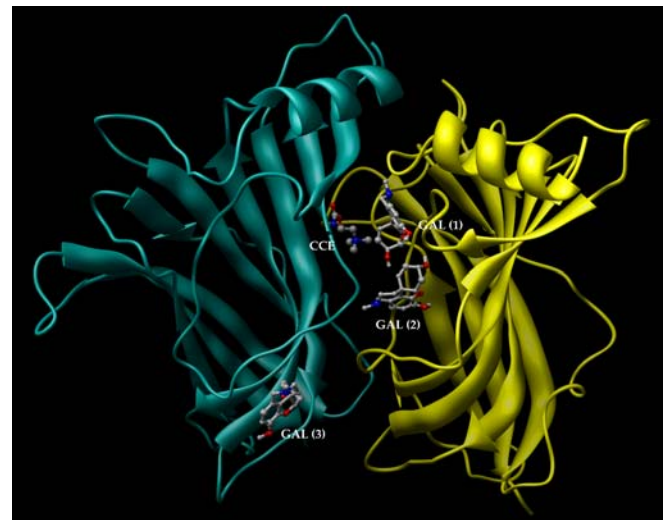


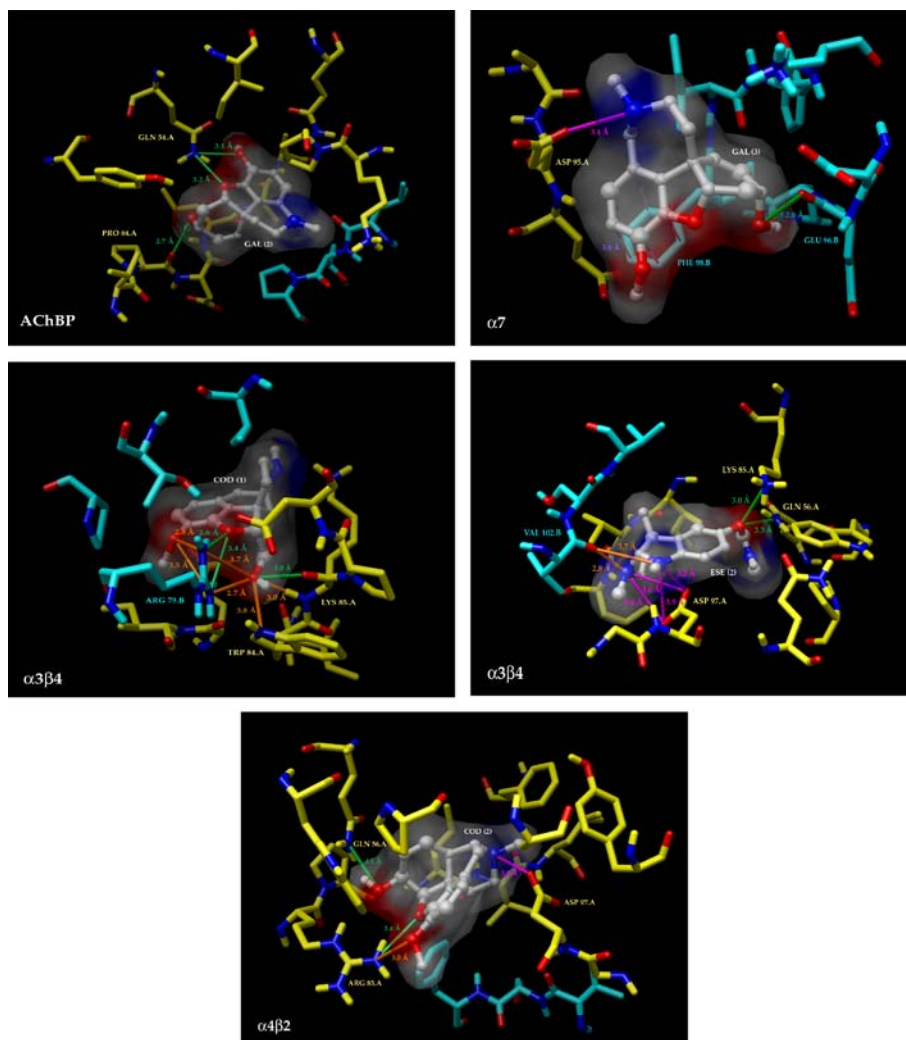
**Fig. 3** Representation of two subunits of AChBP with carbamoylcholine (CCE) in the agonist binding site (PDB entry code 1UW6 [33], back) and galanthamine (GAL) in the putative allosteric binding sites (1, 2 and 3, respectively) found using the “blind docking” approach (front)

positioned close to the L5 loop and  $\beta 7$  and  $\beta 2$  sheets ( $\beta^-$ -subunit) and comprises mainly the residues corresponding to Asp49, Ser93, Lys94, Pro95, Glu96, Arg118, Gln119 and Arg120 ( $\beta^-$  subunit) of AChBP. For more details about the residues composing these three binding sites see Fig. 2 and Tables S1–S3.

An important finding is the location of the first binding site, situated exactly opposite the agonist-binding site, at less than 12 Å through the protein wall. The proximity of these two sites, as well as the high affinity of the ligands for this allosteric site suggest that the allosteric site 1 plays an important role in the potentiation of nAChR. Indeed, the most direct manner to transmit information between two sites is to place them nearby. It must be pointed out that for the first crystallographic structure of AChBP [30] all the seven structural water molecules present in the channel pore observed are located in this allosteric site 1. Additionally, it is worth noting that this high-affinity binding site was found without imposing any constraint and in the absence of water molecules in the docking process.

Some differences in the population of the three sites were observed (Table S4 in supplementary material), depending on the nature of protein and ligand, but two remarks can be made: a) in all cases, the great majority of conformers were found in the sites 1 and 2 and b) the docking energy and the free-binding energy of the conformations found in the third site were always higher than those found in the sites 1 and 2 (Tables S5 and S6 in the supplementary material). As the lack of flexibility in the protein may influence the binding modes of the ligands and the affinities and orientations may importantly vary from one site to another, these results should be considered with care. However, the agonist binding site of acetylcholine nicotinic receptors has been correctly identified previously using AUTODOCK on homology models constructed in a similar manner [41]. The reproducibility observed for all these dockings may suggest that the third site shows an apparent low affinity for the allosteric modulators, in contrast to sites 1 and 2. Considering the position of this third site at the bottom of the ligand binding domain, it might be also implicated in the modulation of the motions needed for opening/closing the narrow ion gate of the

**Fig. 4** Representative binding modes of the most stable docked orientations of galanthamine with AChBP (site 2), galanthamine with human  $\alpha 7$  model (site 3), codeine with human  $\alpha 3\beta 4$  model (site 1), eserine with human  $\alpha 3\beta 4$  model (site 2) and codeine with human  $\alpha 4\beta 2$  model (site 2). See the Supplementary material for several additional examples



transmembrane domain. Additionally, the third site is situated not far from the location previously identified as the allosteric site by photoaffinity labeling [55, 56], and used later for docking studies [45]. However, the experimental protocol used for the photoaffinity labeling (irradiation of nAChR-enriched *Torpedo marmorata* membrane fragments incubated with 8-azidoATP and [<sup>3</sup>H]physostigmine) [55, 56] allows only the identification of allosteric sites located in close proximity to an ATP binding site [75–77].

Several parameters of these three allosteric sites identified by “blind docking” have been calculated (polar and apolar surface areas, volume and depth) and compared with those of the agonist binding site (Table S7 in the supplementary material). The sites are mostly hydrophobic, with some polar regions. Site 1 is rather narrow and deep, similar to the agonist site, whereas sites 2 and 3 are more open and less deep. The third site is smaller than the other ones, and this may explain the weaker affinity of the allosteric ligands observed for this site.

#### “Refined docking”

In the second step, the ligands were docked in each of the three binding sites previously found (“refined docking”). The use of an improved grid resolution allows better evaluation of the protein–ligand interactions, and consequently lower docked energies are obtained with respect to the “blind docking” (see Table S5 in the supplementary material). Fig. 4 shows some representative binding modes of the best docked conformations in the three allosteric sites. Hydrogen bonds were automatically identified using CHIMERA’s “FindHBond” module [64] and the other interactions were identified visually, with a cut-off distance of 4 Å. In most cases, a salt bridge was observed between the positive nitrogen atoms of the ligands and Asp or Glu residues of the protein. Additionally, the oxygen atoms of the ligands were found to be implicated in hydrogen bonds and electrostatic interactions with the protein residues.

On the basis of the results presented above, a possible mechanism for the allosteric activation of the nAChRs can be outlined. We propose the existence of three allosteric binding sites showing different affinities for the allosteric modulators. Since the reversibility of the allosteric modulator binding is generally accepted [53], we can presume an exchange of the ligands between the three allosteric sites. Allosteric binding in the first site probably induces an increase of the agonist binding affinity as a consequence of the proximity of these two sites, which might be connected through a hydrogen-bond network in which protein residues and structural water molecules are involved. On the other hand, despite its apparent low affinity for the ligands, the third site may be implicated in the transmission of the allosteric deformation from the agonist site to the transmembrane domain, due to its key position at the interface between the transmembrane and ligand-binding domains. All these processes will result in an increase of the gate-

opening frequency and the overall potentiation of nAChRs. Additional work is in progress in our laboratory to obtain more information about the exact nature of the interaction between the two adjacent sites, especially the role of the structural water molecules in the activation process. The validation of these results by means of photoaffinity labeling and mutagenesis studies is underway and will be presented elsewhere.

## Conclusions

In the present work we generated models of human  $\alpha 7$ ,  $\alpha 4\beta 2$  and  $\alpha 3\beta 4$  nAChRs by homology modeling, which were docked with three known allosteric modulators of nAChRs using the “blind docking” approach. Three binding sites were identified in the channel pore, one of them being situated in the immediate proximity of the agonist binding site. We propose a possible mechanism for the nAChR activation, which is the first attempt to rationalize this process at the molecular level. Further studies are in progress to investigate the role of crystallographic water molecules in the activation, probably through a hydrogen-bond network. The identification of the allosteric binding site(s) of the nAChRs will subsequently allow the design of new molecules for the treatment of Alzheimer’s disease.

**Acknowledgement** We thank to the Centre National de la Recherche Scientifique (CNRS) for the financial support.

## References

1. Alzheimer A (1906) *Neurolisches Zentralblatt* 25:1134
2. Möller HJ, Graeber MB (1998) *Eur Arch Psychiatry Clin Neurosci* 248:111–122
3. Mattson MP (2004) *Nature* 430:631–639
4. Lane RM, Kivipelto M, Greig NH (2004) *Clin Neuropharmacol* 27:141–149
5. Ibach B, Haen E (2004) *Curr Pharm Des* 10:231–251
6. Rogawski MA, Wenk GL (2003) *CNS Drug Rev* 9:275–308
7. Maelicke A, Schratzenholz A, Samochocki M, Radina M, Albuquerque EX (2000) *Behav Brain Res* 113:199–206
8. Maelicke A (2000) *Dement Geriatr Cogn Disord* 11 Suppl 1: 11–18
9. Maelicke A, Albuquerque EX (2000) *Eur J Pharmacol* 393: 165–170
10. Changeux J, Edelstein SJ (2001) *Curr Opin Neurobiol* 11:369–377
11. Pereira EF, Hilmas C, Santos MD, Alkondon M, Maelicke A, Albuquerque EX (2002) *J Neurobiol* 53:479–500
12. Woodruff-Pak DS, Lander C, Geerts H (2002) *CNS Drug Rev* 8:405–426
13. Geerts H, Finkel L, Carr R, Spiros A (2002) *J Neural Transm Suppl* 203–216
14. Bourin M, Ripoll N, Dailly E (2003) *Curr Med Res Opin* 19: 169–177
15. Doggrell SA, Evans S (2003) *Expert Opin Investig Drugs* 12:1633–1654
16. Romanelli MN, Gualtieri F (2003) *Med Res Rev* 23:393–426
17. Hogg RC, Bertrand D (2004) *Curr Drug Targets CNS Neurol Disord* 3:123–130

18. Maelicke A, Schratzenholz A, Albuquerque EX (2000) In: Clementi F, Fornasari D, Gotti C (eds) *Neuronal nicotinic receptors*. Springer, Berlin, pp 477–496
19. Edelstein SJ, Schaad O, Henry E, Bertrand D, Changeux JP (1996) *Biol Cybern* 75:361–379
20. Unwin N, Miyazawa A, Li J, Fujiyoshi Y (2002) *J Mol Biol* 319:1165–1176
21. Unwin N (2003) *FEBS Lett* 555:91–95
22. Colquhoun D, Unwin D, Shelley C, Hatton C, Sivilotti L (2003) In: Abraham D (ed) *Burger's Medicinal Chemistry*, vol 2, Drug Discovery & Drug Development. Wiley, New York, pp 357–405
23. Grutter T, Le Novere N, Changeux JP (2004) *Curr Top Med Chem* 4:645–650
24. Absalom NL, Lewis TM, Schofield PR (2004) *Exp Physiol* 89:145–153
25. Doyle DA (2004) *Trends Neurosci* 27:298–302
26. Colquhoun D, Sivilotti LG (2004) *Trends Neurosci* 27:337–344
27. Lester HA, Dibas MI, Dahan DS, Leite JF, Dougherty DA (2004) *Trends Neurosci* 27:329–336
28. Miyazawa A, Fujiyoshi Y, Stowell M, Unwin N (1999) *J Mol Biol* 288:765–786
29. Miyazawa A, Fujiyoshi Y, Unwin N (2003) *Nature* 424:949–955
30. Brejc K, van Dijk WJ, Klaassen RV, Schuurmans M, van Der Oost J, Smit AB, Sixma TK (2001) *Nature* 411:269–276
31. Sixma TK, Smit AB (2003) *Annu Rev Biophys Biomol Struct* 32:311–334
32. Smit AB, Brejc K, Syed N, Sixma TK (2003) *Ann NY Acad Sci* 998:81–92
33. Celie PH, van Rossum-Fikkert SE, van Dijk WJ, Brejc K, Smit AB, Sixma TK (2004) *Neuron* 41:907–914
34. Hibbs RE, Talley TT, Taylor P (2004) *J Biol Chem* 279:28483–28491
35. Sine SM (2002) *J Neurobiol* 53:431–446
36. Sine SM, Wang HL, Gao F (2004) *Curr Med Chem* 11:559–567
37. Dutertre S, Lewis RJ (2004) *Eur J Biochem* 271:2327–2334
38. Sine SM, Wang HL, Bren N (2002) *J Biol Chem* 277:29210–29223
39. Molles BE, Tsigelny I, Nguyen PD, Gao SX, Sine SM, Taylor P (2002) *Biochemistry* 41:7895–7906
40. Sullivan D, Chiara DC, Cohen JB (2002) *Mol Pharmacol* 61:463–472
41. Le Novere N, Grutter T, Changeux JP (2002) *Proc Natl Acad Sci USA* 99:3210–3215
42. Yassin L, Samson AO, Halevi S, Eshel M, Treinin M (2002) *Biochemistry* 41:12329–12335
43. Schapira M, Abagyan R, Totrov M (2002) *BMC Struct Biol* 2:1
44. Everhart D, Reiller E, Mirzoiyan A, McIntosh JM, Malhotra A, Luetje CW (2003) *J Pharmacol Exp Ther* 306:664–670
45. Costa V, Nistri A, Cavalli A, Carloni P (2003) *Br J Pharmacol* 140:921–931
46. Henchman RH, Wang HL, Sine SM, Taylor P, McCammon JA (2003) *Biophys J* 85:3007–3018
47. Espinoza-Fonseca LM (2004) *Biochem Biophys Res Commun* 320:587–591
48. Storch A, Schratzenholz A, Cooper JC, Abdel Ghani EM, Gutbrod O, Weber KH, Reinhardt S, Lobron C, Hermsen B, Soskic V, Pereira EFR, Albuquerque EX, Methfessel C, Maelicke A (1995) *Eur J Pharmacol* 290:207–219
49. Schratzenholz A, Pereira EF, Roth U, Weber KH, Albuquerque EX, Maelicke A (1996) *Mol Pharmacol* 49:1–6
50. Maelicke A, Coban T, Storch A, Schratzenholz A, Pereira EF, Albuquerque EX (1997) *J Recept Signal Transduct Res* 17:11–28
51. Lilienfeld S (2002) *CNS Drug Rev* 8:159–176
52. Sabey K, Paradiso K, Zhang J, Steinbach JH (1999) *Mol Pharmacol* 55:58–66
53. Zwart R, van Kleef RG, Gotti C, Smulders CJ, Vijverberg HP (2000) *J Neurochem* 75:2492–2500
54. Arias HR (2000) *Neurochem Int* 36:595–645
55. Schratzenholz A, Coban T, Schroder B, Okonjo KO, Kuhlmann J, Pereira EF, Albuquerque EX, Maelicke A (1993) *J Recept Res* 13:393–412
56. Schratzenholz A, Godovac-Zimmermann J, Schäfer HJ, Albuquerque EX, Maelicke A (1993) *Eur J Biochem* 216:671–677
57. Schroder B, Reinhardt-Maelicke S, Schratzenholz A, McLane KE, Kretschmer A, Conti-Tronconi BM, Maelicke A (1994) *J Biol Chem* 269:10407–10416
58. Ewing TJA, Kuntz ID (1997) *J Comput Chem* 18:1175–1189
59. Hetényi C, van der Spoel D (2002) *Protein Sci* 11:1729–1737
60. Morris GM, Goodsell DS, Halliday RS, Huey R, Hart WE, Belew RK, Olson AJ (1998) *J Comput Chem* 19:1639–1662
61. Thompson JD, Gibson TJ, Plewniak F, Jeanmougin F, Higgins DG (1997) *Nucleic Acids Res* 25:4876–4882
62. Sali A, Blundell TL (1993) *J Mol Biol* 234:779–815
63. Fiser A, Do RK, Sali A (2000) *Protein Sci* 9:1753–1773
64. Pettersen EF, Goddard TD, Huang CC, Couch GS, Greenblatt DM, Meng EC, Ferrin TE (2004) *J Comput Chem* 25:1605–1612
65. Laskowski RA, MacArthur MW, Moss DS, Thornton JM (1993) *J Appl Cryst* 26:283–291
66. Greenblatt HM, Kryger G, Lewis T, Silman I, Sussman JL (1999) *FEBS Lett* 463:321–326
67. Canfield DV, Barrick J, Giessen BC (1987) *Acta Crystallogr, Sect C: Cryst Struct Commun* C43:977–979
68. Pauling P, Petcher TJ (1973) *J Chem Soc, Perkin Trans 2* 1342–1345
69. Sanner MF, Duncan BS, Carrillo CJ, Olson AJ (1999) *Pac Symp Biocomput* 401–412
70. Fraczkiewicz R, Braun W (1998) *J Comput Chem* 19:319–333
71. SYBYL 7.0, Tripos Inc (2004) 1699 South Hanley Road, St. Louis, Missouri, 63144, USA
72. Smit AB, Syed NI, Schaap D, van Minnen J, Klumperman J, Kits KS, Lodder H, van der Schors RC, van Elk R, Sorgedraeger B, Brejc K, Sixma TK, Geraerts WP (2001) *Nature* 411:261–268
73. Fiser A, Sanchez R, Melo F, Sali A (2001) In: Watanabe M, Roux B, MacKerell A, Becker O (eds) *Computational Biochemistry and Biophysics*. Marcel Dekker, New York, pp 275–312
74. Cornell WD, Cieplak P, Bayly CI, Gould IR, Merz KM, Jr., Ferguson DM, Spellmeyer DC, Fox T, Caldwell JW, Kollman PA (1995) *J Am Chem Soc* 117:5179–5197
75. Carlsson BJ, Raftery MA (1993) *Biochemistry* 32:7329–7333
76. Schratzenholz A, Roth U, Schuhen A, Schafer HJ, Godovac-Zimmermann J, Albuquerque EX, Maelicke A (1994) *J Recept Res* 14:197–208
77. Schratzenholz A, Roth U, Godovac-Zimmermann J, Maelicke A (1997) *Biochemistry* 36:13333–13340
78. Chenna R, Sugawara H, Koike T, Lopez R, Gibson TJ, Higgins DG, Thompson JD (2003) *Nucleic Acids Res* 31:3497–3500